

Explanation Multiplicity in SHAP: Characterization and Assessment

HYUNSEUNG HWANG, KAIST, Republic of Korea

SEUNGEUN LEE, New York University, USA

LUCAS ROSENBLATT, New York University, USA

STEVEN EUIJONG WHANG, KAIST, Republic of Korea

JULIA STOYANOVICH, New York University, USA

Post-hoc explanations are widely used to justify, contest, and review automated decisions in high-stakes domains such as lending, employment, and healthcare. Among these methods, SHAP is often treated as providing a reliable account of which features mattered for an individual prediction and is routinely used to support recourse, oversight, and accountability. In practice, however, SHAP explanations can differ substantially across repeated runs, even when the individual, prediction task, and trained model are held fixed.

We conceptualize and name this phenomenon explanation multiplicity: the existence of multiple, internally valid but substantively different explanations for the same decision. Explanation multiplicity poses a normative challenge for responsible AI deployment, as it undermines expectations that explanations can reliably identify the reasons for an adverse outcome. We present a comprehensive methodology for characterizing explanation multiplicity in post-hoc feature attribution methods, disentangling sources arising from model training and selection versus stochasticity intrinsic to the explanation pipeline.

We further show that whether explanation multiplicity is surfaced depends on how explanation consistency is measured. Commonly used magnitude-based metrics can suggest stability while masking substantial instability in the identity and ordering of top-ranked features. To contextualize observed instability, we derive and estimate randomized baseline values under plausible null models, providing a principled reference point for interpreting explanation disagreement. Across datasets, model classes, and confidence regimes, we find that explanation multiplicity is widespread and persists even under highly controlled conditions, including high-confidence predictions. Taken together, these results show that explanation instability is not merely a technical artifact, but a normative concern, and that explanation practices must be evaluated using metrics and baselines aligned with their intended societal role.

1 Introduction

Explainable AI (XAI) has become a central mechanism for justifying and contesting the behavior of machine learning systems deployed in high-stakes domains such as lending, employment, healthcare, and public services [4, 10, 34]. In these settings, post-hoc explanations are routinely used to communicate why a particular decision was made, to support appeals and recourse, and to demonstrate compliance with legal and regulatory requirements. In practice, explanations are often treated not as tentative artifacts of an analysis pipeline, but as authoritative accounts of which features mattered for an individual decision.

Among post-hoc explanation methods, SHAP (SHapley Additive exPlanations) is one of the most widely adopted. SHAP produces local feature attributions based on the Shapley value framework, assigning to each input feature a contribution reflecting its influence on a model’s prediction for a specific individual. These attributions are often treated as a reliable summary of “which features the model used” for a particular prediction [6, 19], and are commonly consumed through ranked lists of “most important” features. As a result, SHAP explanations play a direct role in decision review workflows, algorithmic recourse, and audits of fairness and accountability.

Authors’ Contact Information: Hyunseung Hwang, KAIST, Daejeon, Republic of Korea, aguno@kaist.ac.kr; Seungeun Lee, New York University, New York, NY, USA, seungeun.lee@nyu.edu; Lucas Rosenblatt, New York University, New York, NY, USA, lucas.rosenblatt@nyu.edu; Steven Euijong Whang, KAIST, Daejeon, Republic of Korea, swhang@kaist.ac.kr; Julia Stoyanovich, New York University, New York, NY, USA, stoyanovich@nyu.edu.

Motivating example: explanation disagreement without model disagreement. Consider a binary classifier used to assess credit risk, trained on a fixed dataset and deployed in production. Suppose an individual, Alice, is evaluated by this system and classified as a high-risk applicant, resulting in a loan denial. Alice requests an explanation and is told that the decision was driven primarily by her savings status, employment history, and credit duration (Explainer A in Figure 1). Later, the *same explanation pipeline* is rerun for the same individual, using the same trained model and the same input data. This time, however, the explanation highlights checking account status, existing credit lines, and credit history as the dominant factors (Explainer B in Figure 1). While the predicted outcome remains unchanged, the explanation differs substantially in which features are presented as most important.

From Alice’s perspective, this disagreement is difficult to reconcile. The person is the same, the model is the same, and the decision is the same, yet the explanation shifts. Which explanation should she trust? Which factors should she act on if she seeks recourse or wishes to contest the decision? More broadly, what does it mean for an explanation to be “correct” when multiple, mutually inconsistent explanations can be produced for the same decision? We refer to this phenomenon as **explanation multiplicity**: the existence of multiple, internally valid but substantively different explanations for a single prediction, arising despite the individual, the prediction task, and the trained model being held fixed.

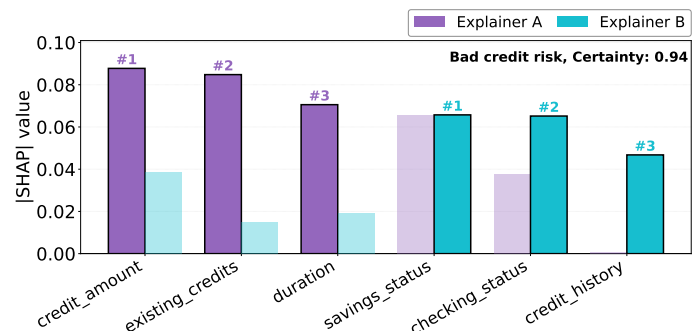


Fig. 1. Instance-level SHAP explanations for a **high-confidence negative prediction** vary substantially when only the explainer setting is changed. The resulting top-ranked features differ across explainers, with no overlap in the top three features, potentially undermining explanation-based decision-making. Example based on lending (German Credit), with an FT-Transformer classifier.

Why explanation multiplicity may arise. At a high level, explanation multiplicity arises because widely used post-hoc explanation methods are implemented as *stochastic approximation pipelines* rather than deterministic mappings from a model and an input to a unique explanation. While Shapley values are uniquely defined in theory [28], computing them exactly is intractable for all but the simplest models, as it requires evaluating the model on all possible coalitions of input features. As a result, practical SHAP implementations rely on sampling-based approximations that introduce randomness into the explanation process.

In particular, popular SHAP estimators such as KernelSHAP [19] and LeverageSHAP [22] approximate feature attributions by repeatedly sampling from a background dataset to simulate feature absence and estimate marginal contributions. Even when the trained model and the input instance are held fixed, different random samples of background data or different internal random seeds can yield different attribution vectors. Consequently, a SHAP explanation should be understood not as a single deterministic object, but as a realization of a random variable induced by the explainer’s approximation procedure.

Explanation multiplicity can also arise from stochasticity elsewhere in the ML pipeline. In many practical settings, models are trained through procedures that involve randomness, such as random initialization, data shuffling, or hyperparameter selection. Different training runs may yield models with comparable predictive performance but

different internal representations and decision boundaries, a phenomenon often described as *model multiplicity* [8]. When explanations are generated for such models, differences in feature attributions may reflect genuine differences in model behavior rather than noise introduced by the explainer.

In practice, these sources of variability are typically entangled. Standard stability analyses often rerun the full explanation pipeline and report aggregate dispersion statistics, without distinguishing whether observed explanation disagreement is driven by differences between trained models or by stochasticity intrinsic to the explainer itself. As a result, explanation multiplicity can be observed even under highly controlled conditions, including settings where the trained model is held fixed and the prediction remains unchanged across runs. This entanglement makes it difficult to attribute observed explanation disagreement to a specific component of the pipeline, motivating closer examination of when and why explanations diverge.

Why consistency is a reasonable expectation, and why its violation matters. The expectation that explanations should be consistent in high-stakes settings is not naive. In many deployment contexts, explanations are presented and consumed as properties of the decision itself rather than as tentative artifacts of a stochastic analysis pipeline [7, 34]. They are used to justify outcomes to affected individuals, to guide human review, and to support institutional accountability, including legal and regulatory oversight [14]. Explanation interfaces rarely disclose randomness or uncertainty, and stakeholders are typically not informed that explanations may vary across runs. As a result, explanation variability directly undermines procedural guarantees that depend on explanations being stable enough to support action, contestation, or oversight [24, 26].

This expectation of consistency mirrors assumptions elsewhere in the machine learning pipeline. While practitioners accept that different training runs may yield different models, it is generally assumed that once a model is fixed, querying it on the same input produces a determinate outcome. Explanations are often implicitly expected to satisfy a similar property: holding the individual, the prediction task, and the trained model fixed, the explanation should not materially disagree about which features mattered [5, 7]. When this expectation is violated, explanation-based mechanisms for transparency, contestability, and accountability become fragile. A system may appear compliant under one explanation and problematic under another, without any change to the underlying model behavior. This ambiguity complicates audits, undermines recourse, and shifts uncertainty onto individuals who are least equipped to resolve it.

Moreover, without disentangling the sources of explanation disagreement, it is difficult to assess whether observed variability reflects meaningful differences in model behavior or merely noise introduced by the explainer itself [3, 8, 35]. This distinction is consequential for governance: variability driven by model multiplicity may warrant changes to training or model selection, whereas variability driven by explainer stochasticity raises more fundamental questions about the suitability of post-hoc explanation tools in high-stakes settings [24, 25].

Surfacing explanation multiplicity: Metrics. Whether explanation multiplicity is detected in practice depends critically on how explanation consistency is measured. Existing work typically evaluates stability by rerunning the explanation pipeline and reporting aggregate dispersion statistics, implicitly treating explanation vectors as objects whose proximity can be summarized by a single magnitude-based score [3, 31]. However, explanations are rarely consumed in this way. In many operational settings, users interact with explanations through ranked lists of the most important features, and downstream actions such as recourse, review, or audit are driven by which features appear at the top rather than by small changes in attribution magnitudes [13].

As a result, different evaluation lenses can lead to qualitatively different conclusions about explanation stability. Aggregate or magnitude-based summaries may suggest that explanations are stable, even when the identity or ordering

of top-ranked features varies substantially across runs. Conversely, metrics that emphasize agreement in feature rankings can reveal pronounced volatility that is obscured by magnitude-based measures [23]. Making explanation multiplicity visible therefore requires metrics that align with how explanations are interpreted and acted upon in practice. In this work, we show that metric choice is not merely a technical detail, but a central factor in determining whether explanation instability is surfaced or systematically masked. This paper makes the following contributions:

1: Explanation multiplicity as a first-class concept. We conceptualize and name *explanation multiplicity*: the phenomenon in which multiple, internally valid but substantively different explanations are produced for the same individual decision, even when the prediction task and trained model are held fixed. By foregrounding explanation multiplicity as a distinct object of study, we separate it from related notions such as model multiplicity and explanation robustness, and frame it as a first-order concern for responsible AI deployment.

2: A comprehensive methodology for assessing explanation multiplicity in post-hoc feature attribution methods. Our methodology systematically probes explanation variability across repeated runs and explicitly disentangles sources of multiplicity arising from model training and selection versus stochasticity intrinsic to the explanation pipeline. This dissection enables principled interpretation of explanation disagreement and clarifies when instability reflects genuine differences in model behavior versus artifacts of the explainer.

3: Metrics and baselines for surfacing explanation multiplicity. We show that whether explanation multiplicity is detected depends critically on how explanation consistency is measured. We study both magnitude-based and rank-based metrics and demonstrate that commonly used aggregate summaries can mask substantial instability in the identity and ordering of top-ranked features. To contextualize observed variability, we derive and estimate randomized baseline values under plausible null models, providing a reference point for assessing when explanation disagreement is meaningfully larger than what would be expected by chance.

4: Empirical evidence across models, datasets, and confidence regimes. Through an extensive empirical study spanning multiple datasets, model classes, and explanation settings, we demonstrate that explanation multiplicity is widespread and persists even under highly controlled conditions. We show that the dominant source of multiplicity depends on the data regime and model class, and that high-confidence predictions do not guarantee stable explanations.

2 Related Work

Our work builds on and connects several lines of research on post-hoc explanations, sources of explanation variability, and the evaluation of explanation consistency.

Stochasticity in post-hoc explanations. Explanation methods such as LIME [25] and SHAP [19] are widely used, yet their behavior under stochastic approximation has been repeatedly questioned. Zhang et al. [35] model LIME explanations as random variables and propose increasing the number of samples to reduce variance, though the suggested sample sizes can be impractical for large datasets. Visani et al. [31] similarly document explanation variability in LIME and recommend averaging explanations across many runs to increase consistency.

More recent work has focused on the role of the SHAP background dataset. Yuan et al. [33] empirically study the effect of background data size on SHAP variability and suggest using large background sets to reduce disagreement across runs. Aivodji et al. [2] demonstrate that manipulating the background data can deliberately suppress feature importance while preserving marginal data distributions, highlighting the sensitivity of SHAP explanations to background selection. In contrast, Musco and Witter [22] propose leverage-score sampling to improve the accuracy of SHAP estimation within a fixed background dataset. While these works address explainer stochasticity, they focus primarily on improving estimation procedures rather than characterizing explanation disagreement across repeated runs.

Metrics for explanation consistency. A wide range of metrics has been proposed to quantify explanation consistency across runs. Common approaches rely on magnitude-based distances such as ℓ_2 distance between explanation vectors [31], while others adopt rank-based measures such as Jaccard distance [23]. Slack et al. [29] propose a Bayesian framework for SHAP that yields confidence intervals for feature attributions, explicitly acknowledging explanation uncertainty. However, their evaluation relies on magnitude-based summaries and does not address disagreement in feature rankings that are most commonly used in practice. Large benchmarks such as OpenXAI [1] report multiple metrics across explainers, but typically present raw values or standard deviations without contextualizing them against any baseline. Our work departs from this literature by showing that metric choice fundamentally shapes whether explanation multiplicity is surfaced or masked. In particular, we demonstrate that magnitude-based metrics can suggest consistency even when rank-based metrics reveal substantial disagreement relative to randomized baselines. We further contribute a baseline calibration framework that enables interpretation of observed disagreement relative to plausible null models.

Prediction confidence and explanation consistency. Several studies have examined the relationship between predictive uncertainty and explanation consistency. Shaikhina et al. [27] and Zhu et al. [36] show that explanations for low-confidence predictions tend to exhibit greater variability, leading to the common intuition that explanation instability is primarily a concern near decision boundaries. However, these analyses focus on uncertainty in predictions rather than explanation disagreement under repeated runs. Our work complements and extends this literature by evaluating explanation multiplicity conditioned on prediction confidence, while holding predictions fixed. We show that high-confidence predictions do not guarantee consistent explanations, and that explainer-induced stochasticity alone can produce substantial rank disagreement even when the model output is nearly deterministic.

Model multiplicity versus explanation multiplicity. Explanation variability can also arise from differences in the underlying model. The notion of *model multiplicity*, or the Rashomon effect [9], captures the fact that many models can achieve similar predictive performance while relying on different features. Marx et al. [21] show that changing model seeds can lead to different predictions, and Black et al. [8] demonstrate that retraining neural networks can yield different counterfactual explanations even when trained on the same data. Recent work has begun to distinguish model-induced variability from data-induced variability. Hwang et al. [18] show that SHAP explanations are sensitive to feature representation choices even when the model is held fixed. Our current work builds on this distinction by explicitly disentangling variability due to model training and selection from variability introduced by stochastic explanation pipelines, and by framing this separation through the lens of *explanation multiplicity*.

In summary, in contrast to prior work that focuses on improving estimation procedures, increasing sample sizes, or reporting uncalibrated metrics, we introduce explanation multiplicity as a first-class concept and provide a framework for characterizing and assessing it. By disentangling sources of variability and calibrating metrics against randomized baselines, our work provides a systematic basis for interpreting explanation disagreement in high-stakes settings.

3 Preliminaries

The Shapley value [28] is widely used to quantify local feature importance in predictive classification [11, 19], particularly to measure how much each feature contributes to black-box model predictions. It assesses how changes to a feature’s value, on its own or in combination with other features, impact an outcome. Formally,

$$\phi_i(f) = \sum_{S \subseteq N \setminus \{i\}} \frac{|S|!(|N| - |S| - 1)!}{|N|!} (f(S \cup \{i\}) - f(S)) \quad (1)$$

Here, the features are the entities whose contributions are being measured and f is the predictive model. We refer to the assignment of Shapley values (equivalently, “weights” or “contributions”) to a sample’s features as an *explanation*. The magnitude of a Shapley value reflects how a feature influences the prediction, while its sign indicates the direction of that influence. High Shapley values assigned to protected attributes such as age or race indicate that these features play a substantial role in the decision, which may raise ethical or legal concerns.

In principle, Shapley values are uniquely defined for a given model and input instance. The Shapley value of a feature is obtained by averaging its marginal contribution to the model output over all possible subsets of the remaining features, weighted by subset size, as formalized in (1). This definition yields a single, well-defined attribution vector over features that satisfies desirable axioms such as efficiency, symmetry, linearity, and the null-player property [19, 28].

Computing Shapley values exactly, however, is computationally infeasible for all but the simplest models. Exact computation requires evaluating the model on all 2^{d-1} subsets of features for each feature, resulting in exponential time complexity in the number of input features d . Consequently, practical implementations like SHAP [19], which we use in this work, rely on approximation techniques to estimate Shapley values, replacing exact enumeration with sampling-based procedures that trade computational tractability for statistical approximation accuracy.

Stochasticity in SHAP values from background sampling. Practical explanation methods like SHAP [19] approximate true Shapley values using *background sampling*. They estimate marginal contributions with respect to a background distribution, so changing the background dataset changes the distribution being approximated.

To illustrate this mechanism, consider three features: *payment_history* (ph), *savings_amount* (sa), and *loan_size* (ls). Let x describe an applicant with ph = good, sa = low, and ls = high. When estimating the contribution of ph , SHAP compares the model’s prediction with ph present to predictions in which ph is treated as missing. Since the model requires all features to be specified, missing values are filled in by drawing from a background dataset.

Concretely, for a coalition $S \subseteq N \setminus \{i\}$, SHAP estimates

$$\hat{f}(x_S; D_{bg}) = \mathbb{E}_{Z_{N \setminus S} \sim D_{bg}} [f(x_S, Z_{N \setminus S})],$$

where x_S denotes feature values taken from the instance x and $Z_{N \setminus S}$ denotes values for the remaining features drawn from the background dataset D_{bg} . Because these expectations are approximated via sampling, the resulting SHAP attributions are stochastic: repeated runs with different D_{bg} can produce different explanations for the same (x, f) .

4 Defining and Assessing Explanation Multiplicity

4.1 What is Explanation Multiplicity

We consider a standard post-hoc explanation setting with a trained predictive model and an explanation procedure. Let $\mathcal{X} \subseteq \mathbb{R}^d$ denote the input space, and let $f : \mathcal{X} \rightarrow \mathbb{R}$ (or $f : \mathcal{X} \rightarrow [0, 1]$ for probabilistic classification) denote the model. An *explainer* is a procedure \mathcal{E} that, given a model f and an instance $x \in \mathcal{X}$, returns a feature-importance explanation $\phi(x) = \mathcal{E}(f, x) \in \mathbb{R}^d$, where each coordinate represents a feature’s contribution to the prediction at x .¹

In many deployment settings, explanations are treated as properties of a decision for a fixed individual. The input record x is fixed, the prediction task is fixed, and the explanation is expected to provide a stable account of which features mattered for the outcome. However, as discussed in Section 3, practical explanation pipelines may involve stochastic components. As a result, repeated executions of the same explanation query can yield different feature-importance

¹Throughout, we use “feature-importance explanation” to refer to local post-hoc attributions or rankings; the definition below does not assume a specific attribution formalism.

explanations, even when the input instance x and the prediction outcome are held fixed. We formalize this phenomenon as a property of an *explanation query*, rather than of a single model or explainer run.

Definition (Explanation multiplicity). An *explanation query* consists of (i) a dataset and prediction task, (ii) a target instance x , and (iii) a choice of model class and explainer family. We say that *explanation multiplicity* occurs if repeated executions of the same explanation query can produce multiple, substantively different feature-importance explanations for the same data point. Here, “the same explanation query” means that the dataset, prediction task, model class, and explainer family are held fixed, and repeated executions differ only through stochastic choices internal to the modeling-and-explanation pipeline.

4.2 Assessing Explanation Multiplicity

To assess explanation multiplicity in practice, we introduce a *methodology* based on controlled reruns of the same modeling-and-explanation workflow. This methodology enables us to systematically probe explanation multiplicity and disentangle variability arising from model construction versus stochasticity intrinsic to the explanation pipeline. Figure 2 illustrates a SHAP-style explanation pipeline and highlights the points at which multiplicity can arise. Assessing explanation multiplicity requires not only generating multiple explanations under controlled conditions, but also selecting appropriate metrics to quantify and interpret their disagreement; we introduce these metrics and their calibration in Section 5.

Explanation pipeline and sources of multiplicity. Given a dataset and prediction task, the pipeline proceeds as follows: (1) split the data into training and test sets, (2) train a model f using a fixed model class and training protocol, and (3) generate a feature-importance explanation for a fixed test instance x using a SHAP estimator. The explainer represents missing features by sampling from a background dataset \mathcal{D}_{bg} drawn from the training data. Even when the explanation query is held fixed, this pipeline can yield multiple, substantively different explanations because randomness may enter at two distinct stages: *model construction*, where rerunning the same training-and-selection procedure can produce different trained models, and *explanation*, where practical SHAP estimators rely on stochastic approximation.

Dual-seed protocol. To disentangle sources of explanation multiplicity, we parameterize each execution by two

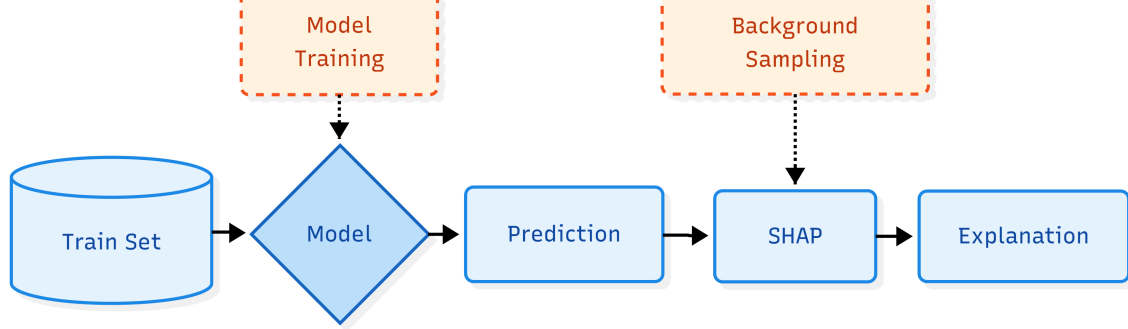


Fig. 2. **Explanation pipeline and sources of explanation multiplicity.** Randomness can enter at (a) model construction (training and selection) and (b) explanation (stochastic SHAP approximation, e.g., background resampling), yielding multiple explanations for the same instance.

random seeds. Let $\phi(x; s_m, s_e) \in \mathbb{R}^d$ denote the SHAP explanation for instance x obtained from a run indexed by a

Manuscript submitted to ACM

model seed s_m and an explainer seed s_e . Seed s_m controls randomness in training and model selection, while s_e controls stochasticity intrinsic to the SHAP approximation. By varying (s_m, s_e) while holding the dataset, prediction task, model class, and explainer family fixed, we obtain multiple realizations of $\phi(x)$ for the same explanation query.

Multiplicity settings. Using the dual-seed formulation, we assess explanation multiplicity under three complementary settings: **(i) Overall multiplicity**, rerunning the full modeling-and-explanation pipeline end-to-end; **(ii) model-induced multiplicity**, rerunning training and selection while holding the explainer fixed; and **(iii) explainer-induced multiplicity**, holding the trained model fixed and rerunning SHAP while varying only explainer stochasticity, primarily through resampling \mathcal{D}_{bg} . In all settings, each pipeline execution yields a single feature-importance vector for the same instance x . Explanation multiplicity is quantified by measuring pairwise disagreement among the resulting explanations. Section 5 introduces the disagreement metrics and randomized baselines that complete the assessment framework by determining when observed explanation disagreement is meaningfully large.

5 Metrics and baselines for surfacing explanation multiplicity

This section addresses a natural and lingering question: when is explanation multiplicity meaningfully large, and when is it merely noise? Because SHAP explanations are produced by stochastic approximation pipelines, some degree of variation across runs is expected. The challenge is therefore not to detect variation per se, but to determine when observed explanation disagreement exceeds what would plausibly arise from randomness alone.

To answer this question, we introduce an *interpretive infrastructure* for explanation multiplicity. Specifically, we show that whether multiplicity is surfaced or masked depends critically on the choice of evaluation metric and on the availability of calibrated reference baselines. We therefore present a hierarchy of metrics and randomized null models that together determine when explanation disagreement should be considered substantively significant rather than incidental. These metrics and baselines complement the source disentanglement protocol introduced in Section 4.2 by providing the means to interpret the magnitude and relevance of disagreement once its origin has been isolated, and are used throughout the empirical evaluation in Section 6.

5.1 Evaluation Metrics

To interpret explanation multiplicity, we evaluate disagreement between explanations using a hierarchy of metrics that emphasize different aspects of feature-importance variation, ranging from magnitude-based to rank-based measures and finally to feature-level granularity. Each metric captures a distinct notion of disagreement, and as we show, some lenses systematically mask explanation multiplicity while others reveal it.

1. ℓ_2 Distance. The most common metric for instability is the Euclidean distance between explanation vectors. For two different SHAP vectors $\phi_i \in \mathbb{R}^d$ and $\phi_j \in \mathbb{R}^d$,

$$D_{\ell_2}(\phi_i, \phi_j) = \|\phi_i - \phi_j\|_2 \quad (2)$$

While ℓ_2 captures the magnitude of change, it is insensitive to rank permutations. A small D_{ℓ_2} can still result in a different set of top features, creating an “illusion of stability.” Thus, ℓ_2 distance can mask explanation multiplicity that is salient for stakeholders who rely on ranked feature importance rather than absolute attribution magnitudes.

2. Top- k Jaccard Distance. Because explanations are often consumed through a small set of top-ranked features, we also consider rank-set disagreement. Stakeholders often rely on the top- k most important features for decision-making. Let π_i and π_j denote the rankings induced by $|\phi_i|$ and $|\phi_j|$, respectively. We write π_i^k and π_j^k for the sets of feature

indices appearing in the top- k positions of these rankings. The top- k Jaccard distance is defined as:

$$D_{\text{Jac}}(\pi_i, \pi_j) = 1 - \frac{|\pi_i^k \cap \pi_j^k|}{|\pi_i^k \cup \pi_j^k|}. \quad (3)$$

A value of 0 indicates identical top- k sets, while 1 indicates disjoint sets.

3. Rank-Biased Overlap (RBO). Top- k Jaccard ignores ordering within the top set. We therefore also report Rank-Biased Overlap (RBO) [32], a top-weighted similarity between ranked lists. At depth ℓ , let $A_\ell = |\pi_i^{1:\ell} \cap \pi_j^{1:\ell}|/\ell$. We define the RBO-based sensitivity as

$$S_{\text{RBO}}(\pi_i, \pi_j) = 1 - \left[(1-p) \sum_{\ell=1}^d p^{\ell-1} A_\ell + p^d A_d \right], \quad (4)$$

where $p \in (0, 1)$ controls top-heaviness (smaller p emphasizes higher ranks). Unlike top- k Jaccard, RBO downweights disagreements deeper in the ranking, making it sensitive to whether instability occurs among the most salient features or further down the list.

4. Feature-wise Sensitivity (diagnostic view). Global metrics like ℓ_2 or RBO aggregate stability into a single scalar, potentially masking that specific features are disproportionately unstable. To capture this nuance, we measure the **Mean Pairwise Distance** for each feature m . Given a set of N explanations generated under different seeds, this metric computes the average absolute difference between all distinct pairs of SHAP values for that feature:

$$S_{\text{feat}}^{(m)} = \frac{1}{N(N-1)} \sum_{i \neq j} \left| \phi_i^{(m)} - \phi_j^{(m)} \right| \quad (5)$$

This metric allows us to construct a *Vulnerability Map*, identifying which features drive instability by quantifying their fluctuation magnitude across runs. This feature-wise view helps explain why aggregate metrics may disagree by revealing which features drive explanation multiplicity and where small fluctuations can reorder rankings.

5.2 Baseline Sensitivity under Randomized Nulls

Observed explanation disagreement values are difficult to interpret in isolation. For example, a top- k Jaccard distance of 0.4 may indicate substantial explanation multiplicity, or it may be indistinguishable from disagreement expected under random variation. Without a reference point, it is therefore unclear when explanation disagreement should be considered meaningfully large rather than incidental. To address this, we introduce randomized null models that provide calibrated reference ranges for each metric. These baselines are not treated as ground truth; rather, they serve as interpretive yardsticks against which observed explanation disagreement can be evaluated.

5.2.1 ℓ_2 Distance. We begin with a randomized baseline for magnitude-based disagreement that preserves the overall scale of SHAP attributions while randomizing their allocation across features.

Given two SHAP vectors $\phi \in \mathbb{R}^d$ and $\phi' \in \mathbb{R}^d$, let $T := \sum_{i=1}^d |\phi_i|$. We model a randomized SHAP magnitude vector as $X := TM$, where M is drawn from a Dirichlet distribution over the probability simplex Δ^{d-1} , so that M distributes the fixed total mass T across features. We define $Y := TM'$ analogously. The Dirichlet distribution allocates a fixed total mass across components, making it a natural random model for distributing the nonnegative magnitudes of SHAP values across feature dimensions while preserving their overall scale. The full specification of this randomized null model is given in Appendix A.1.

PROPOSITION 5.1 (EXPECTED SQUARED ℓ_2 DISTANCE). *Let X, Y be drawn i.i.d. from the model in Appendix A.1. Then*

$$\mathbb{E} \|X - Y\|_2^2 = \frac{2T^2}{\kappa + 1} \left(1 - \frac{\rho^2}{k} - \frac{(1 - \rho)^2}{d - k}\right). \quad (6)$$

Here, k denotes the cardinality of the top- k feature set. A detailed proof and the definitions of κ and ρ are in Appendix A.1.

This expectation provides a reference scale for ℓ_2 disagreement under random allocation of attribution mass, allowing observed values to be interpreted relative to chance.

5.2.2 Top- k Jaccard Distance and Rank-biased Overlap (RBO). For rank-based metrics, we require a null model that captures plausible variability in ranked feature importance while retaining a shared latent ordering. We use a Mallows model under Kendall-Tau distance [20] as a probabilistic null for SHAP feature rankings (see Appendix A.2).

The Mallows model generates rankings by perturbing a common latent ordering, making it a principled reference distribution for rank-based stability metrics such as top- k Jaccard and RBO. For a rank-based functional $f \in \{D_{\text{Jac}}, S_{\text{RBO}}\}$, we define the Mallows baseline as:

$$B_f(q) = \mathbb{E}_{\pi, \pi' \sim \text{Mallows}(e, q)} [f(\pi, \pi')], \quad (7)$$

where $e = (1, \dots, d)$ is the identity permutation and the dispersion parameter $q \in (0, 1)$. Details of the Mallows model are given in Appendix A.2. Since a closed-form expression for (7) is not available, we estimate it via Monte Carlo sampling using N samples:

$$\widehat{B}_f(q) = \frac{1}{N} \sum_{t=1}^N f(\pi^{(t)}, \pi'^{(t)}), \quad \pi^{(t)}, \pi'^{(t)} \sim \text{Mallows}(e, q).$$

Randomized baselines require specifying hyperparameters of the underlying stochastic models. For the Dirichlet baseline, these include the fraction ρ of total mass assigned to the top- k features and the concentration parameter κ (see Appendix A.1), while the Mallows baseline is parameterized by a single dispersion parameter q (see Appendix A.2). We visualize nulls as shaded bands rather than single lines to reflect uncertainty in the null and avoid over-interpreting small deviations from an arbitrary reference. These bands capture the range of baselines induced by sweeping over plausible hyperparameter settings. In contrast to the ℓ_2 , which involves multiple parameters, the ranking-based baseline depends on a single parameter and therefore admits a more constrained and realistic calibration range.

6 Empirical Evaluation

We empirically investigate explanation multiplicity in SHAP values, guided by three questions: **Source of multiplicity**: When explanations disagree across repeated runs, is this disagreement primarily attributable to variability in the trained model, or to stochasticity intrinsic to the explanation method itself? **Visibility under metrics**: Under which evaluation choices is explanation multiplicity surfaced versus masked? **Role of confidence**: Is high prediction confidence sufficient to warrant treating explanations as stable?

To address these questions, we conduct three analyses. (1) We measure overall multiplicity and then *dissect* it into model-induced and explainer-induced components to identify the dominant source of disagreement across dataset–model regimes. (2) We evaluate multiplicity under a hierarchy of comparison metrics (magnitude-, rank-, and set-based) and use a feature-wise instability analysis (Section 5) to diagnose which parts of the importance landscape (e.g., near-ties versus volatile top features) drive metric divergence. (3) We stratify instances by prediction confidence and reassess multiplicity under fixed predictions (explainer-induced setting); we additionally report feature-wise instability within each confidence group to test whether the same unstable features persist even for high-confidence decisions.

6.1 Experimental Setup

Datasets. We evaluate three tabular datasets spanning different scales: ACS Income (Virginia, 2018) [12] ($N=45,960, d=8$), German Credit [16] ($N=988, d=16$), and Diabetes [30] ($N=392, d=8$), with the corresponding classification tasks. We use stratified 5-fold cross-validation: compute sensitivity instance-wise on each test fold, then aggregate across folds.

Models. To avoid model-specific conclusions, we consider diverse predictors: tree-based (DT, RF, XGB), neural (MLP, FT-Transformer [15]), and prior-data fitted (TabPFN [17]). Trainable models are tuned via grid search within each outer fold; TabPFN is used without tuning (details in Appendix A.4).

SHAP configuration. We compute SHAP on prediction probabilities and sample the background dataset \mathcal{D}_{bg} uniformly from the training split ($K=100$ for ACS Income and German Credit; $K=50$ for Diabetes).

6.2 Identifying the Source of Explanation Multiplicity

To identify the source of explanation multiplicity, we decompose it into two components: *model-induced* and *explainer-induced*. Using the dual-seed protocol, we measure *model-induced multiplicity* by varying the model random seed while fixing the explainer, and *explainer-induced multiplicity* by varying the explainer seed while fixing the trained model. Figure 3 summarizes this decomposition across datasets and evaluation metrics.

Dataset size and multiplicity regimes. We observe a clear regime-dependent pattern. For smaller datasets such as German Credit and Diabetes, explanation multiplicity is primarily model-induced. This behavior reflects the limited training data in these settings, which prevents convergence to a unique model and leads to diverse predictive behaviors across runs. In contrast, for the large-scale ACS Income, explainer-induced multiplicity dominates. Here, trained models are relatively stable across runs, but explanation disagreement remains substantial due to stochastic approximation in SHAP. While the large training set stabilizes the model, the explainer relies on a limited background dataset to approximate Shapley values. In high-dimensional settings such as ACS Income, this background sample provides only a coarse summary of the underlying data distribution, causing approximation error in the explanation method to become the primary source of explanation multiplicity.

Multiplicity across model families. Across datasets, neural architectures exhibit higher explanation multiplicity than tree-based models and TabPFN. This pattern is consistent with the greater sensitivity of neural models to training initialization and complex decision boundaries. TabPFN, which relies on a fixed prior-data fitting procedure rather than retraining, exhibits comparatively lower explanation multiplicity. Overall, while model class influences the magnitude of explanation multiplicity, the dominant source—model-induced versus explainer-induced—is primarily determined by the dataset regime rather than the model family.

In summary, the dominant source of explanation multiplicity is context-dependent: in small-data regimes it is primarily model-induced; in large-scale settings explainer-induced multiplicity can dominate despite stable models.

6.3 Metric Divergence and Feature Landscape Analysis

Across all evaluated models and datasets, rank-based metrics exhibit substantially higher explanation multiplicity than magnitude-based ℓ_2 , often approaching randomized baseline levels, while RBO lies between these extremes. Figure 4 illustrates why rank-based multiplicity persists even when ℓ_2 variation is low, by showing how SHAP attribution variability is distributed across feature ranks.

This divergence is driven by the underlying *feature-importance landscape*. In German Credit, the top-ranked feature is dominant, but the subsequent features form a flat plateau with nearly indistinguishable importance values. Small

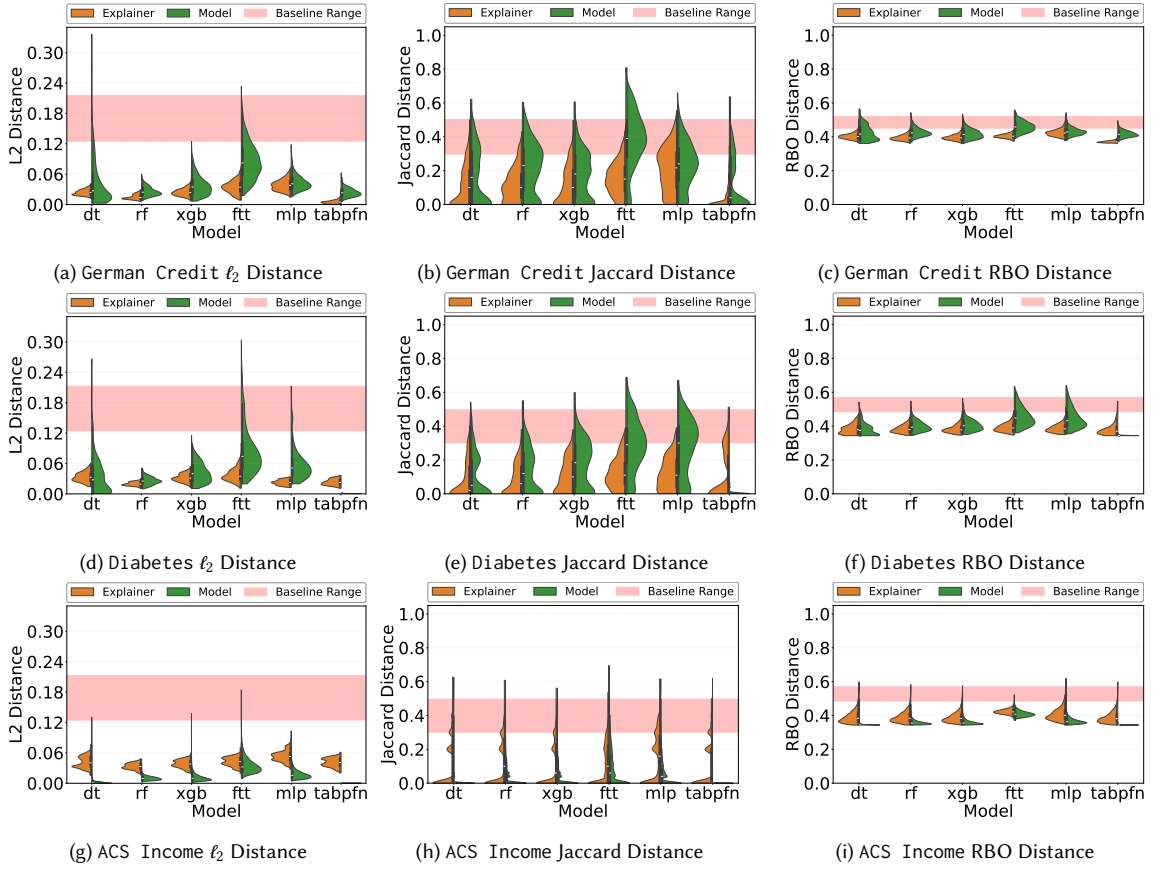


Fig. 3. Model vs. explainer multiplicity (dissection). Violin plots decomposed by the source of randomness across three datasets (rows) and three metrics (columns: ℓ_2 , Top- k Jaccard, and RBO). Orange violins vary only the explainer seed with the model fixed; green violins vary the model seed with the explainer fixed. Shaded bands denote randomized baseline ranges. German Credit and Diabetes show predominantly model-induced multiplicity, whereas ACS Income exhibits stronger explainer-induced multiplicity.

fluctuations introduced by the explainer are therefore sufficient to reorder these features, yielding high top- k Jaccard multiplicity despite a stable leading feature. In Diabetes, a similar pattern appears in the mid-ranked features, where near-ties among ranks 3–5 make the top- k set highly susceptible to random reordering. In contrast, ACS Income exhibits a volatile core: although there is a clear separation between the top-ranked features and the tail, the top features themselves show high variability, leading to frequent swaps or exclusions and pronounced rank-based multiplicity.

Overall, ℓ_2 distance masks structural sources of explanation multiplicity by averaging over attribution magnitudes. In contrast, Jaccard distance surfaces practice-relevant multiplicity by capturing instability in the top- k feature set, whether driven by flat tails or volatile top features. RBO offers a complementary, rank-aware view but is less sensitive to top- k membership changes because it aggregates agreement over ranked prefixes. Since explanations are typically consumed through a small set of top-ranked features, auditing top- k multiplicity is critical.

In summary, whether explanation multiplicity is visible or hidden depends critically on the evaluation metric: magnitude-based measures can mask substantial disagreement that is readily surfaced by rank-based metrics aligned with how explanations are used in practice.

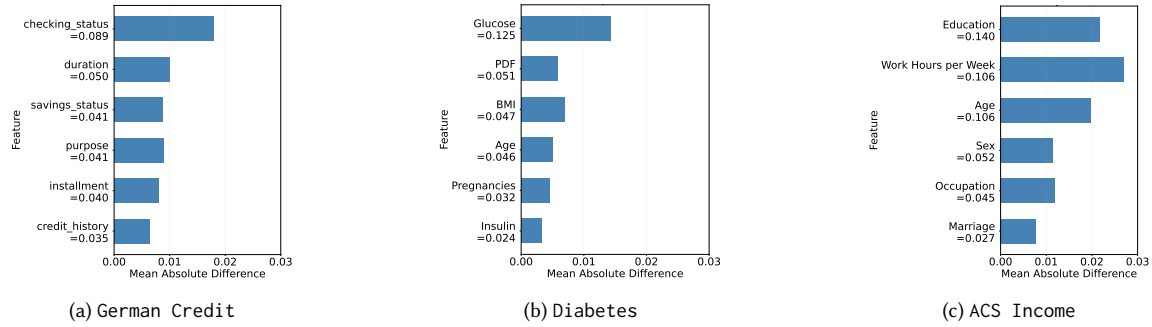


Fig. 4. **Explainer-seed feature-wise multiplicity.** With the model fixed, we vary the explainer seed and report feature-level explanation multiplicity for top features. Bar length shows mean pairwise attribution change; annotations indicate average importance.

6.4 Independence from Prediction Confidence

Finally, we examine whether prediction confidence provides a reliable signal of explanation multiplicity. In this experiment, we stratify instances by predicted probability into *Certain* ($P > 0.9$ or $P < 0.1$) and *Uncertain* ($0.4 \leq P \leq 0.6$). To isolate explanation variability, we fix the trained model and vary only the explainer seed. Intuitively, one might expect explanations for high-confidence predictions to be more stable than those near the decision boundary. Our results Figure 6 and 7 in the appendix partially support this intuition: explanations for uncertain instances exhibit higher absolute explanation multiplicity. However, prediction confidence alone is not a reliable indicator of explanation stability. Even for instances with high predicted probability, explanation multiplicity remains non-negligible. This behavior reflects a scale effect in feature attributions. While absolute fluctuations in SHAP values are smaller for confident predictions, average attribution magnitudes are also reduced. As a result, even minor variation introduced by the explainer can reorder features with similar importance, leading to persistent rank-based explanation multiplicity. Consequently, metrics such as top- k Jaccard remain elevated, often near randomized baseline levels, even when predictions are highly confident.

In summary, high prediction confidence does not guarantee low explanation multiplicity; even confident predictions can exhibit substantial disagreement, see Appendix A.5 for additional results.

7 Discussion

This work highlights a broader implication for responsible AI practice: *the evaluation of explanations is not a neutral technical exercise, but a normative choice that shapes what kinds of failures become visible*. Across datasets, models, and evaluation lenses, we find that explanation multiplicity is often present even when conventional stability metrics suggest robustness. This discrepancy, which we describe as an *illusion of stability*, arises from a mismatch between how explanations are evaluated and how they are used in practice.

Evaluation choices shape what counts as stable. In many high-stakes settings, explanations are consumed as ranked lists of features that inform downstream actions such as recourse, review, and auditing. Yet evaluation practices often assess stability using aggregate, magnitude-based metrics such as ℓ_2 distance, which treat explanations as numerical vectors rather than decision-facing artifacts. Our results show that such metrics can mask substantial disagreement in the identity and ordering of top-ranked features, whereas rank-based metrics surface explanation multiplicity aligned with practical use. This contrast highlights that metric choice encodes assumptions about what aspects of explanations matter, and that misalignment between evaluation and use can obscure salient risks.

Explainers as part of decision-making infrastructure. A second implication concerns the role of the explainer itself. We find that explanation multiplicity is often driven not by model variability, but by stochasticity intrinsic to the explanation pipeline, particularly in large-scale data regimes. This challenges the assumption that explanation disagreement primarily reflects model uncertainty. Instead, explainers should be treated as components of decision-making infrastructure with their own convergence properties and failure modes, and focusing evaluation solely on model robustness or prediction confidence can leave explanation behavior under-scrutinized.

From detecting variation to interpreting significance. Explanation pipelines that rely on approximation or sampling inevitably exhibit variability. The practical question is not whether variation exists, but when it is meaningfully large. By introducing randomized baselines, we show how explanation disagreement can be interpreted, not just reported, making explicit the assumptions under which explanation multiplicity is judged acceptable or concerning.

Implications beyond SHAP. While our empirical analysis focuses on SHAP, the broader lesson is not method-specific. Many post-hoc explanation techniques rely on approximation or sampling that introduce variability. Normative risk arises when such variability is ignored or evaluated using metrics that do not reflect how explanations are consumed, motivating a socio-technical view of explanation evaluation.

8 Conclusions, Limitations, and Future Work

This paper shows that explanation multiplicity is a pervasive property of post-hoc explanation pipelines and that its visibility depends critically on how explanations are evaluated. Magnitude-based metrics can suggest stability even when rank-based disagreement is substantial, creating an illusion of stability that is misaligned with how explanations are used in practice. By disentangling model-induced and explainer-induced sources of explanation multiplicity and introducing calibrated baselines, our work reframes explanation evaluation as an interpretive task rather than a purely descriptive one, highlighting the need for evaluation practices that align with downstream use, acknowledge stochasticity, and provide meaningful reference points in high-stakes settings.

This study has several limitations. First, our analysis of SHAP relies on a fixed background sample size due to computational constraints. While prior work suggests that increasing the background dataset can reduce explanation variability [33], we restrict our experiments to a standard sampling budget (e.g., 100 samples), reflecting common resource constraints in practice. Our findings therefore characterize explanation multiplicity under realistic, but not exhaustive, background sampling regimes. Second, the randomized baselines introduced in this work rely on empirical estimates of distributional parameters derived from observed SHAP values rather than ground-truth generative models. Our goal is not to recover a true distribution, but to provide calibrated reference points for interpreting explanation disagreement. We view these baselines as pragmatic yardsticks that improve upon interpreting stability metrics in isolation, and note that the framework is modular and could be refined in future work to incorporate richer distributional assumptions or feature dependencies.

Several directions for future work emerge from our findings. Extending the proposed evaluation framework to explanation methods beyond SHAP would help assess the generality of explanation multiplicity across post-hoc approaches. Exploring adaptive or data-dependent background sampling may clarify how explainer-induced multiplicity can be mitigated in large-scale settings. An additional open challenge is how explanation variability should be communicated to non-expert stakeholders without overwhelming them. Finally, integrating calibrated explanation evaluation into deployment and governance workflows, such as model validation or monitoring, represents a promising path for translating these insights into practice.

9 Generative AI Usage Statement

Generative AI tools (namely, ChatGPT 5.2) were used in a limited capacity to support editing and refinement of the manuscript text, including improving clarity, organization, and phrasing. All technical content, experimental design, data analysis, results, and interpretations are the authors' own. Generative AI tools were not used to generate experimental results, figures, tables, or to make scientific claims.

10 Ethical Considerations Statement

This work raises ethical considerations about how post-hoc explanations are interpreted and used in high-stakes decision contexts. In practice, explanation outputs are often presented as authoritative accounts of model behavior, even though they may depend on stochastic approximation and evaluation choices that are not disclosed to affected individuals.

The ethical risk is not explanation variability itself, but the potential for explanations to be over-interpreted when their sensitivity is ignored or obscured. When a single explanation is treated as definitive without appropriate context, stakeholders may place unwarranted confidence in it, with implications for procedural fairness, contestability, and accountability.

Our experiments use only publicly available benchmark datasets and do not involve human subjects or real-world deployment. Nonetheless, the findings underscore the importance of cautious interpretation. When explanations are used to support decisions affecting individuals' rights or opportunities, variability should be acknowledged and evaluation assumptions made explicit.

While this study focuses on SHAP, similar concerns may apply to other post-hoc explanation methods that rely on approximation or sampling. Future work should explore responsible ways to communicate explanation variability to non-expert stakeholders.

Acknowledgments

This work was supported in part by the NYU-KAIST Partnership and by the Institute of Information & Communications Technology Planning & Evaluation (IITP) with a grant funded by the Ministry of Science and ICT (MSIT) of the Republic of Korea in connection with the Global AI Frontier Lab International Collaborative Research. (No. RS-2024-00469482 & RS-2024-00509258). This work was also supported in part by US National Science Foundation (NSF) Awards No. 2312930, 2326193, and NSF GRFP DGE-2234660, and by the National Research Foundation of Korea (NRF) grant funded by the Korea government (MSIT) (No. RS-2022-NR070121).

References

- [1] Chirag Agarwal, Satyapriya Krishna, Eshika Saxena, Martin Pawelczyk, Nari Johnson, Isha Puri, Marinka Zitnik, and Himabindu Lakkaraju. 2022. OpenXAI: Towards a Transparent Evaluation of Model Explanations. In *Thirty-sixth Conference on Neural Information Processing Systems Datasets and Benchmarks Track*.
- [2] Ulrich Aïvodji, Satoshi Hara, Mario Marchand, Foutse Khomh, et al. 2023. Fooling shap with stealthily biased sampling. In *The Eleventh International Conference on Learning Representations*.
- [3] David Alvarez-Melis and Tommi S Jaakkola. 2018. On the robustness of interpretability methods. *arXiv preprint arXiv:1806.08049* (2018).
- [4] Sarah Alwarthan, Nida Aslam, and Irfan Ullah Khan. 2022. An explainable model for identifying at-risk student at higher education. *IEEE Access* 10 (2022), 107649–107668.
- [5] Solon Barocas, Moritz Hardt, and Arvind Narayanan. 2023. *Fairness and Machine Learning: Limitations and Opportunities*. MIT Press, Cambridge, MA.
- [6] Adrien Bennetot, Ivan Donadello, Ayoub El Qadi El Haouari, Mauro Dragoni, Thomas Frossard, Benedikt Wagner, Anna Sarranti, Silvia Tulli, Maria Trocan, Raja Chatila, et al. 2024. A practical tutorial on explainable AI techniques. *Comput. Surveys* 57, 2 (2024), 1–44.

- [7] Umang Bhatt, Alice Xiang, Shubham Sharma, Adrian Weller, Ankur Taly, Yunhan Jia, Joydeep Ghosh, Ruchir Puri, José M. F. Moura, and Peter Eckersley. 2020. Explainable Machine Learning in Deployment. In *Proceedings of the 2020 Conference on Fairness, Accountability, and Transparency (FAccT)*. ACM, 648–657.
- [8] Emily Black, Manish Raghavan, and Solon Barocas. 2022. Model Multiplicity: Opportunities, Concerns, and Solutions. In *Proceedings of the 2022 ACM Conference on Fairness, Accountability, and Transparency (FAccT '22)*. Association for Computing Machinery, New York, NY, USA, 850–863. doi:10.1145/3531146.3533149
- [9] Leo Breiman. 2001. Statistical Modeling: The Two Cultures (with comments and a rejoinder by the author). *Statist. Sci.* 16, 3 (2001), 199 – 231. doi:10.1214/ss/1009213726
- [10] Ahmad Chaddad, Jihao Peng, Jian Xu, and Ahmed Bouridane. 2023. Survey of explainable AI techniques in healthcare. *Sensors* 23, 2 (2023), 634.
- [11] Anupama Datta, Shayak Sen, and Yair Zick. 2016. Algorithmic Transparency via Quantitative Input Influence: Theory and Experiments with Learning Systems. In *IEEE Symposium on Security and Privacy, SP 2016, San Jose, CA, USA, May 22–26, 2016*. IEEE Computer Society, 598–617. doi:10.1109/SP.2016.42
- [12] Frances Ding, Moritz Hardt, John Miller, and Ludwig Schmidt. 2021. Retiring Adult: New Datasets for Fair Machine Learning. *Advances in Neural Information Processing Systems* 34 (2021).
- [13] João Fonseca, Andrew Bell, Carlo Abrate, Francesco Bonchi, and Julia Stoyanovich. 2023. Setting the right expectations: Algorithmic recourse over time. In *Proceedings of the 3rd ACM Conference on Equity and Access in Algorithms, Mechanisms, and Optimization*. 1–11.
- [14] Benjamin Fresz, Elena Dubovitskaya, Danilo Brajovic, Marco F. Huber, and Christian Horz. 2024. How Should AI Decisions Be Explained? Requirements for Explanations from the Perspective of European Law. In *Proceedings of the AAAI/ACM Conference on AI, Ethics, and Society (AIES)*. ACM, 438–450.
- [15] Yury Gorishniy, Ivan Rubachev, Valentin Khrulkov, and Artem Babenko. 2021. Revisiting deep learning models for tabular data. *Advances in neural information processing systems* 34 (2021), 18932–18943.
- [16] Hans Hofmann. 1994. Statlog (German Credit Data). UCI Machine Learning Repository. DOI: <https://doi.org/10.24432/C5WG6W>.
- [17] Noah Hollmann, Samuel G. Müller, Katharina Eggensperger, and Frank Hutter. 2022. TabPFN: A Transformer That Solves Small Tabular Classification Problems in a Second. In *International Conference on Learning Representations*.
- [18] Hyunseung Hwang, Andrew Bell, Joao Fonseca, Venetia Pliatsika, Julia Stoyanovich, and Steven Euijong Whang. 2025. SHAP-based Explanations are Sensitive to Feature Representation. In *Proceedings of the 2025 ACM Conference on Fairness, Accountability, and Transparency*. 1588–1601.
- [19] Scott M Lundberg and Su-In Lee. 2017. A unified approach to interpreting model predictions. *Advances in neural information processing systems* 30 (2017).
- [20] Colin L Mallows. 1957. Non-null ranking models. I. *Biometrika* 44, 1/2 (1957), 114–130.
- [21] Charles Marx, Flavio Calmon, and Berk Ustun. 2020. Predictive multiplicity in classification. In *International conference on machine learning*. PMLR, 6765–6774.
- [22] Christopher Musco and R Teal Witter. 2025. Provably Accurate Shapley Value Estimation via Leverage Score Sampling. In *International Conference on Learning Representations*.
- [23] Sarah Nogueira, Konstantinos Sechidis, and Gavin Brown. 2017. On the stability of feature selection algorithms. *The Journal of Machine Learning Research* 18, 1 (2017), 6345–6398.
- [24] Samir Passi and Solon Barocas. 2019. Problem Formulation and Fairness. In *Proceedings of the 2019 Conference on Fairness, Accountability, and Transparency (FAT*)*. ACM, 39–48.
- [25] Marco Tulio Ribeiro, Sameer Singh, and Carlos Guestrin. 2016. "Why should I trust you?" Explaining the predictions of any classifier. In *Proceedings of the 22nd ACM SIGKDD international conference on knowledge discovery and data mining*. 1135–1144.
- [26] Andrew D. Selbst, Danah Boyd, Sorelle A. Friedler, Suresh Venkatasubramanian, and Janet Vertesi. 2019. Fairness and Abstraction in Sociotechnical Systems. In *Proceedings of the 2019 Conference on Fairness, Accountability, and Transparency (FAT*)*. ACM, 59–68.
- [27] Torgyn Shaikhina, Umang Bhatt, Roxanne Zhang, Konstantinos Georgatzis, Alice Xiang, and Adrian Weller. 2021. Effects of uncertainty on the quality of feature importance explanations. In *AAAI workshop on explainable agency in artificial intelligence*. AAAI Press.
- [28] Lloyd S Shapley et al. 1953. A value for n-person games. (1953).
- [29] Dylan Slack, Anna Hilgard, Sameer Singh, and Himabindu Lakkaraju. 2021. Reliable post hoc explanations: Modeling uncertainty in explainability. *Advances in neural information processing systems* 34 (2021), 9391–9404.
- [30] Jack W Smith, Johannes E Everhart, WC Dickson, William C Knowler, and RS Johannes. 1988. Using the ADAP learning algorithm to forecast the onset of diabetes mellitus. In *Proceedings of the Annual Symposium on Computer Application in Medical Care*. American Medical Informatics Association, 261.
- [31] Giorgio Visani, Enrico Bagli, Federico Chesani, Alessandro Poluzzi, and Davide Capuzzo. 2022. Statistical stability indices for LIME: Obtaining reliable explanations for machine learning models. *Journal of the Operational Research Society* 73, 1 (2022), 91–101. doi:10.1080/01605682.2020.1865846
- [32] William Webber, Alistair Moffat, and Justin Zobel. 2010. A similarity measure for indefinite rankings. *ACM Transactions on Information Systems (TOIS)* 28, 4 (2010), 1–38.
- [33] Han Yuan, Mingxuan Liu, Lican Kang, Chenkui Miao, and Ying Wu. 2023. An Empirical Study of the Effect of Background Data Size on the Stability of SHapley Additive exPlanations (SHAP) for Deep Learning Models.

- [34] Leid Zejnilovic, Susana Lavado, Carlos Soares, Íñigo Martínez De Rituerto De Troya, Andrew Bell, and Rayid Ghani. 2021. Machine learning informed decision-making with interpreted model's outputs: A field intervention. In *Academy of Management Proceedings*, Vol. 2021. Academy of Management Briarcliff Manor, NY 10510, 15424.
- [35] Yujia Zhang, Kuangyan Song, Yiming Sun, Sarah Tan, and Madeleine Udell. 2019. "Why Should You Trust My Explanation?" Understanding Uncertainty in LIME Explanations. arXiv:1904.12991 [cs.LG]
- [36] Chenrui Zhu, Louenias Bounia, Vu Linh Nguyen, Sébastien Destercke, and Arthur Hoarau. 2025. Robust Explanations Through Uncertainty Decomposition: A Path to Trustworthier AI. arXiv:2507.12913 [cs.LG]

A Appendix

A.1 Proof of Proposition 5.1

Proof. To define a baseline structure, we fix an index set $S \subset [d] = \{1, 2, \dots, d\}$ with $|S| = k$ containing top- k features. Let $\rho \in [0, 1]$ denote the fraction of total mass assigned to the top- k features, i.e., the cumulative importance carried by indices in S . We define a baseline mean composition $m \in \Delta^{d-1}$ by allocating a total mass of ρ to the top- k features and $1 - \rho$ to the remaining $d - k$ features, and distributing the mass uniformly within each group. Formally, the baseline mean vector m is defined component-wise as:

$$m_i = \begin{cases} \rho/k, & i \in S, \\ (1 - \rho)/(d - k), & i \notin S. \end{cases} \quad (8)$$

We model M as a Dirichlet random vector,

$$M \sim \text{Dirichlet}(\alpha), \quad \alpha_i = \kappa m_i > 0 \quad \forall i,$$

where $\kappa > 0$ is a concentration parameter. Smaller values of κ induce heavier-tailed and sparser realizations, while larger values concentrate mass more tightly around the mean m . We adopt a Dirichlet distribution because it models random nonnegative vectors on the probability simplex under a unit-sum constraint, which matches the normalized absolute SHAP explanation vectors.

Since X and Y are i.i.d.,

$$\mathbb{E} \|X - Y\|_2^2 = 2 \text{tr}(\text{Cov}(X)).$$

We have

$$\text{Cov}(X) = T^2 \text{Cov}(M)$$

as $X = TM$, and thus

$$\mathbb{E} \|X - Y\|_2^2 = 2T^2 \text{tr}(\text{Cov}(M)).$$

For a Dirichlet(α) distribution with $\alpha_0 = \sum_i \alpha_i = \kappa$ and $m_i = \alpha_i/\alpha_0$,

$$\text{Var}(M_i) = \frac{m_i(1 - m_i)}{\kappa + 1}, \quad (9)$$

$$\text{Cov}(M_i, M_j) = -\frac{m_i m_j}{\kappa + 1}, \quad i \neq j. \quad (10)$$

Therefore,

$$\text{tr}(\text{Cov}(M)) = \sum_{i=1}^d \text{Var}(M_i) = \frac{1 - \sum_{i=1}^d m_i^2}{\kappa + 1}.$$

From equation (8),

$$\sum_{i=1}^d m_i^2 = k \left(\frac{\rho}{k} \right)^2 + (d - k) \left(\frac{1 - \rho}{d - k} \right)^2 = \frac{\rho^2}{k} + \frac{(1 - \rho)^2}{d - k}.$$

With $\alpha_0 = \kappa$, we obtain

$$\text{tr}(\text{Cov}(M)) = \frac{1}{\kappa + 1} \left(1 - \frac{\rho^2}{k} - \frac{(1 - \rho)^2}{d - k} \right).$$

Multiplying by $2T^2$ completes the proof. \square

It is noteworthy that while d , k , and T are determined by the explanation setting (with $k = 3$ throughout our experiments and $T = 0.4$ based on its empirical average), the parameters ρ and κ are hyperparameters required to

stantiate a baseline distribution. Empirically, we find that $\rho \approx 0.7$ and $\kappa \approx 10$ roughly match the scale of observed SHAP value distributions. We treat this as a central reference point while varying $\rho \in \{0.6, 0.7, 0.8\}$ and $\kappa \in \{5, 6, \dots, 15\}$ to ensure our findings are robust to calibration choices and not dependent on precise parameter values. Importantly, we use these parameters only to define a plausible perturbation regime. The baseline remains an independent stochastic process that reflects how much explanations could vary.

A.2 Mallows model under Kendall-Tau distance

Definition A.1 (Mallows model under Kendall-Tau distance [20]). Let \mathcal{S}_d denote the set of all permutations of $[d]$, representing rankings of d features, and let d_{KT} be the Kendall-Tau distance (i.e., the number of pairwise inversions between two permutations) on \mathcal{S}_d . For a central ranking $\pi_0 \in \mathcal{S}_d$ and a dispersion parameter $q \in [0, 1)$, the *Mallows model* on \mathcal{S}_d is defined as:

$$\mathbb{P}(\pi \mid \pi_0, q) = \frac{q^{d_{\text{KT}}(\pi, \pi_0)}}{Z_d(q)}, \quad Z_d(q) = \sum_{\sigma \in \mathcal{S}_d} q^{d_{\text{KT}}(\sigma, e)}, \quad (11)$$

where $e = (1, 2, \dots, d)$ denotes the identity permutation.

We first sample a central ranking $\pi_0 \sim \text{Unif}(\mathcal{S}_d)$. Conditioned on π_0 , we then generate two ranking permutations centered at π_0 as follows:

$$\pi, \pi' \stackrel{\text{i.i.d.}}{\sim} \text{Mallows}(\pi_0, q),$$

where q controls the magnitude of the perturbations. This construction defines a *shared-center null model*: π and π' are conditionally independent given π_0 , but marginally dependent through the common latent ranking. Compared to the hypergeometric distribution, which assumes uniformly random top- r sets, the shared-center Mallows model provides a controlled and more realistic stochastic variability.

For any ranking-based functional $f : \mathcal{S}_d \times \mathcal{S}_d \rightarrow \mathbb{R}$ (e.g., Jaccard distance and Rank-biased Overlap (RBO)), we define the Mallows baseline as:

$$B_f(q) := \mathbb{E}_{\pi_0} \mathbb{E}_{\pi, \pi' \mid \pi_0} [f(\pi, \pi')]. \quad (12)$$

Since all quantities of interest are invariant to the choice of the central ranking π_0 , the baseline simplifies to

$$B_f(q) = \mathbb{E}_{\pi, \pi' \sim \text{Mallows}(e, q)} [f(\pi, \pi')]. \quad (13)$$

In practice, the expectation in (13) is approximated via Monte Carlo sampling.

As in the ℓ_2 baseline, the dimensionality d and $k = 3$ are fixed by the experimental settings. For the RBO-based ranking baseline, we set $p = 1 - 1/d$, where d is the number of features, so that the expected effective comparison depth, $1/(1 - p)$, spans the full feature ranking. All baselines are estimated using $N = 20,000$ Monte Carlo samples, which is sufficient to ensure stable estimates.

The hyperparameter used to instantiate the ranking-based baseline is the Mallows dispersion parameter q . Empirically, we find that $q \approx 0.4$ matches the scale of observed variability, and we therefore consider $q \in \{0.3, 0.4, 0.5\}$ to capture a range of plausible randomness levels. In contrast to the ℓ_2 baseline (5.1), which requires calibrating multiple parameters, the ranking-based baseline depends on a single dispersion parameter. This results in a more constrained and tractable calibration space, and consequently a narrower and more realistic range of randomized baselines.

A.3 Feature-level SHAP under preprocessing pipelines

Motivation. Our goal is to audit stability at the level of *semantic input features* (e.g., race, occupation), rather than at the level of post-encoding dimensions. In tabular modeling practice, categorical variables are frequently one-hot encoded prior to training. Running SHAP directly on one-hot dimensions splits a single semantic feature into many binary indicators, complicating interpretation and downstream auditing. More importantly for perturbation-based explainers, independently masking or sampling one-hot dimensions may violate mutual-exclusivity constraints (e.g., multiple category indicators active simultaneously), producing coalitions that are not meaningful in the original feature space and potentially distorting attribution comparisons.

Pipeline design. To preserve the training-time preprocessing while producing feature-level explanations, we implement the predictor as an `sklearn Pipeline`:

$$f(x) = g(T(x)),$$

where x is the original (pre-encoded) tabular input, T is a deterministic preprocessing transform (e.g., one-hot encoding and scaling), and g is the learned model. All models in our study are trained and evaluated through the same interface, so that SHAP queries operate on the same feature schema across heterogeneous predictors.

Why a model-agnostic explainer. This pipeline-centric design supports consistent, feature-level auditing across heterogeneous model classes (trees, ensembles, and neural networks) without re-implementing feature-grouping logic separately per model-specific explainer. While model-specific SHAP implementations can be more computationally efficient under certain assumptions, using a single model-agnostic explainer avoids confounding differences in explanation backends and ensures that all sensitivity comparisons are performed under the same perturbation semantics and interface. Accordingly, we use KernelSHAP throughout the paper.

Reproducibility details. We keep the preprocessing transform T fixed once trained, and we sample the background dataset \mathcal{D}_{bg} from the corresponding training split. The only randomness introduced by the explainer is the background sampling and the internal sampling used by KernelSHAP, which we control via explicit seeds in our experimental protocol (Section 6.1).

A.4 Hyperparameter Optimization

For all models (except TabPFN, which is pre-trained), we performed hyperparameter tuning within each fold of the outer cross-validation loop. To reduce computational cost while maintaining robustness, we employed a validation set strategy using `ShuffleSplit` (1 split, test size = 0.2, random state = 0) rather than full inner cross-validation. The best hyperparameter configuration was selected based on the **ROC-AUC** score.

Table 1 summarizes the fixed parameters and the grid search space for each model. Note that TabPFN was used without fine-tuning as it is a prior-data fitted network designed for inference on tabular data.

Table 1. **Hyperparameter Search Space.** Fixed parameters are set to ensure fair comparison or convergence, while grid parameters are optimized using a validation set.

Model	Fixed Parameters	Grid Search Parameters (Values)
Decision Tree	-	<code>max_depth</code> $\in \{3, 5, \text{None}\}$ <code>min_samples_leaf</code> $\in \{1, 5, 10\}$
Random Forest	<code>n_estimators</code> = 200	<code>max_depth</code> $\in \{\text{None}, 7, 15\}$ <code>min_samples_leaf</code> $\in \{1, 5\}$
XGBoost	<code>n_estimators</code> = 200 <code>tree_method</code> = ‘hist’ <code>eval_metric</code> = ‘logloss’	<code>max_depth</code> $\in \{3, 5\}$ <code>learning_rate</code> $\in \{0.05, 0.1\}$ <code>subsample</code> $\in \{0.8, 1.0\}$
FT-Transformer	<code>attn_heads</code> = 8 <code>dropout</code> = 0.1 <code>optimizer</code> = AdamW	<code>d_block</code> $\in \{64, 128\}$ <code>n_blocks</code> $\in \{2, 3\}$ <code>lr</code> $\in \{1e-4, 3e-4\}$
MLP	<code>activation</code> = ReLU <code>batch_size</code> = 256 <code>epochs</code> = 100	<code>hidden_dims</code> $\in \{(64), (128), (128, 64)\}$ <code>lr</code> $\in \{1e-3, 3e-4\}$ <code>weight_decay</code> $\in \{1e-4, 1e-3\}$ <code>dropout</code> $\in \{0.0, 0.1\}$
TabPFN	Pre-trained Model	<i>No hyperparameter tuning performed.</i>

A.5 Additional Experimental Results

This appendix reports experimental results that were omitted from the main text due to space limits. Across all plots, sensitivities are computed over repeated runs under the same *explanation query* (i.e., fixed test instance and model checkpoint when applicable), and shaded bands indicate the ranges induced by our randomized baselines.

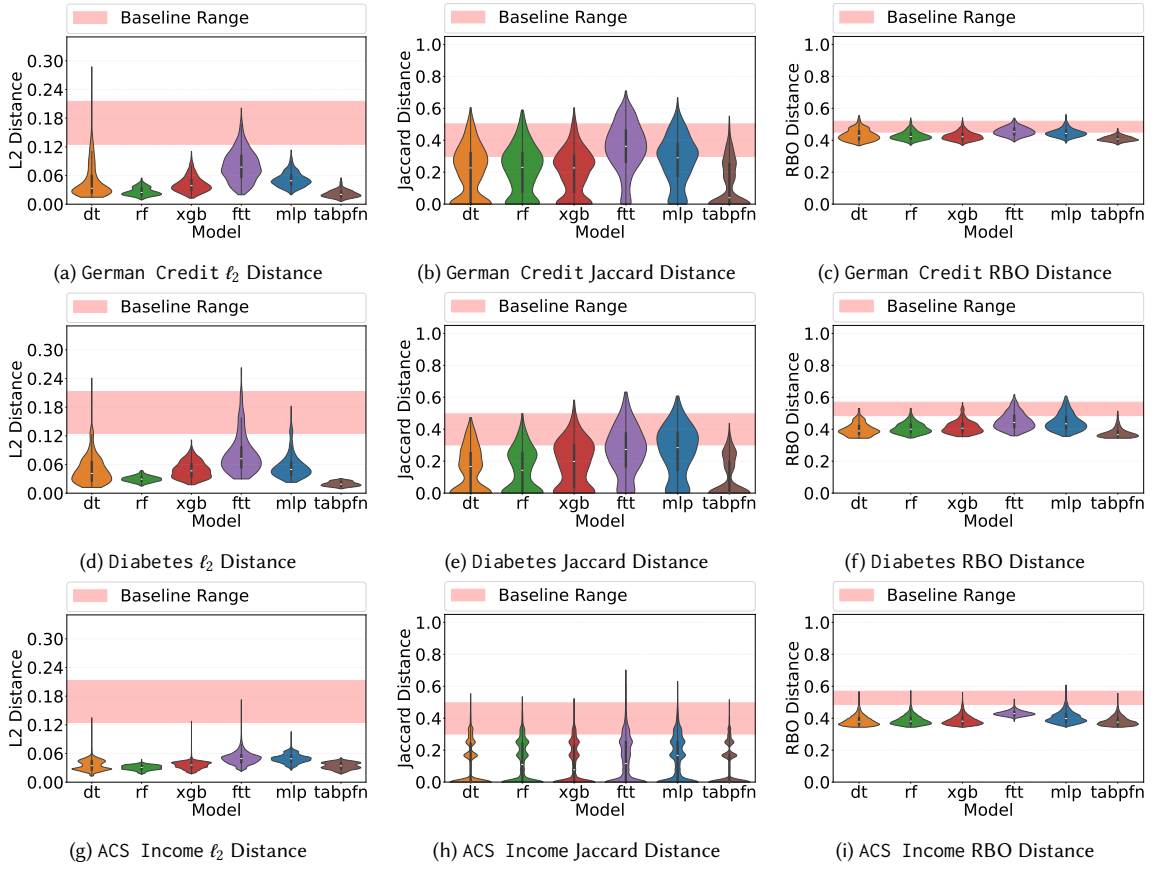


Fig. 5. Diabetes and ACS Income overall sensitivity. Violin plots of overall sensitivity across repeated runs for Diabetes (top row) and ACS Income (bottom row), measured by ℓ_2 , Top- k Jaccard, and RBO distances. Shaded bands indicate randomized baseline ranges. FT-Transformer and MLP exhibit Jaccard sensitivity approaching the baseline, whereas ℓ_2 remains concentrated near zero across models. Notably, ACS Income shows multimodal Jaccard distributions, including a dense low-sensitivity mass and additional modes closer to the baseline.

Overall sensitivity distributions. Figure 5 visualizes the distribution of *overall sensitivity* across repeated runs for German Credit, Diabetes, and ACS Income using three metrics (ℓ_2 , Top- k Jaccard, and RBO). Consistent with the main text, ℓ_2 distances often concentrate near zero even when rank-based metrics show substantial instability, highlighting an *illusion of stability* when only magnitude-based metrics are reported. We also observe multimodality in some rank-based distributions (notably on ACS Income), suggesting the existence of multiple recurring explanation modes for the same query.

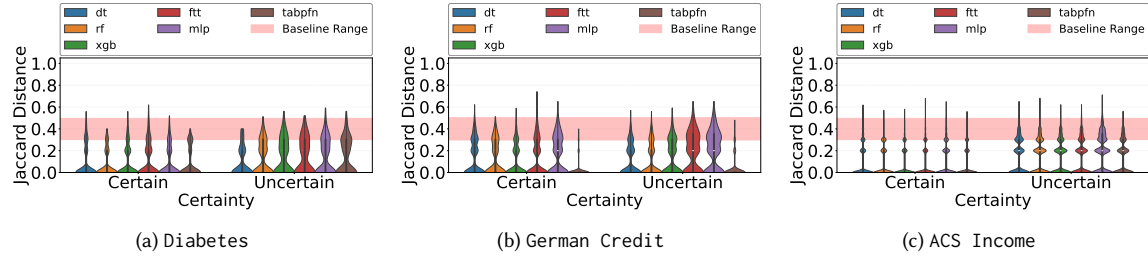


Fig. 6. Confidence vs. stability. Jaccard sensitivity distributions for *certain* and *uncertain* predictions (stratified by predicted probability), computed under the *explainer-sensitivity* setting where the model is held fixed and only the explainer seed is varied. Shaded bands denote randomized baselines. Uncertain predictions are often more sensitive, but high-confidence predictions can still exhibit substantial instability.

Prediction confidence vs. stability. Figure 6 examines whether explanation stability is aligned with prediction confidence under the *explainer-sensitivity* setting (model fixed; only the explainer seed varies). We stratify test instances into *certain* predictions (e.g., $p \geq 0.9$ or $p \leq 0.1$) and *uncertain* predictions (e.g., $0.4 \leq p \leq 0.6$), where p denotes the model’s predicted probability. Uncertain predictions tend to be more sensitive on average; however, high-confidence predictions can still exhibit non-trivial rank instability relative to the randomized baselines.

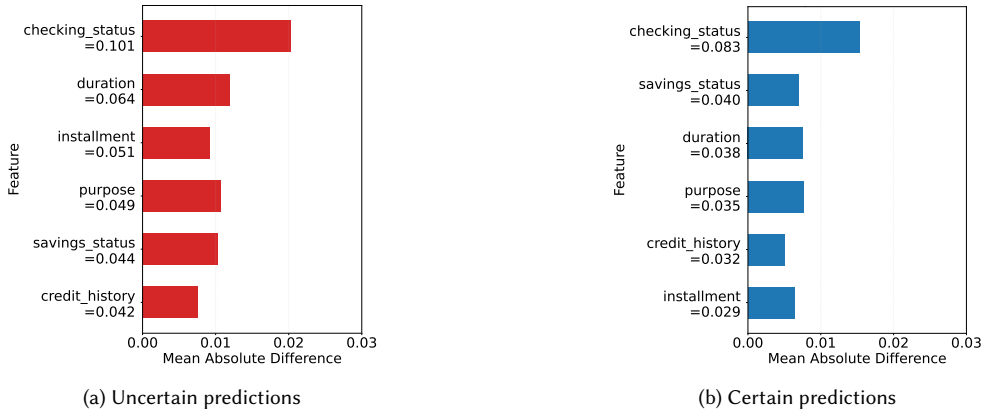


Fig. 7. Feature-wise sensitivity under certain and uncertain predictions (German Credit). Feature-level instability when varying only the explainer seed, shown separately for uncertain (left) and certain (right) predictions. Uncertain predictions exhibit larger absolute fluctuations, but certain predictions can still experience rank-order churn because average attributions are smaller, so even modest noise is sufficient to swap nearby features.

Feature-wise sensitivity under certainty stratification. To explain why high-confidence predictions may still show rank-order churn, Figure 7 reports feature-wise sensitivity for German Credit (MLP) under uncertain vs. certain predictions. Uncertain predictions typically have larger absolute fluctuations, whereas certain predictions often have smaller average attributions; consequently, even modest noise can swap nearby features and lead to rank instability despite small ℓ_2 changes.